

Electron Transfer in a Radical Ion Pair: Quantum Calculations of the Solvent Reorganization Energy

Marco Caricato,^{*,†} Francesca Ingrosso,^{*,‡} Benedetta Mennucci,[†] and Hirofumi Sato[§]

Dipartimento di Chimica e Chimica Industriale, Università di Pisa, Via Risorgimento 26, 56126 Pisa, Italy, CNRS UMR 8640 Pasteur, Département de Chimie, École Normale Supérieure, 24 Rue Lhomond, 75231 Paris Cedex 05, France, and Department of Molecular Engineering, Kyoto University, Kyoto 615-8510, Japan

Received: May 26, 2006; In Final Form: August 31, 2006

Results are presented for an investigation of intermolecular electron transfer (ET) in solution by means of quantum calculations. The two molecules that are involved in the ET reaction form a solvent-separated radical ion pair. The solvent plays an important role in the ET between the two molecules. In particular, it can give rise to specific solute–solvent interactions with the solutes. An example of specific interactions is the formation of a hydrogen bond between a protic solvent and one of the molecules involved in the ET. We address the study of this system by means of quantum calculations on the solutes immersed in a continuum solvent. However, when the solvent can give rise to hydrogen bond formation with the negatively charged ion after ET, we explicitly consider solvent molecules in the solute cavity, determining the hydrogen bond energetic contribution to the overall interaction energy. Solute–solvent pair distribution functions, showing the different arrangement of solvent molecules before and after ET in the first solvation shell, are reported. We provide results of the solvent reorganization energy from quantum calculations for both the two isolated fragments and the ion pair in solution. Results are in agreement with available experimental data.

1. Introduction

Electron transfer (ET) in solution is one of the most widely studied processes in chemistry, from both the experimental and the theoretical/computational points of view. One of the crucial quantities to appreciate solvent effects on ET (or more in general on charge transfers) is the solvent reorganization energy. Any charge transfer between two molecules in solution requires a significant rearrangement of the solvent molecules around each of the two reactants; hence, it costs a great deal of the solvent polarization energy. This energy penalty for disrupting the local solvent structure is defined as the solvent reorganization energy, λ_s .

Using the well-known Marcus formula,¹ such an energy can be calculated by knowing the static (ϵ) and the optical (ϵ_∞) dielectric permittivity of the solvent, namely

$$\lambda_s^M = \left(\frac{1}{2d_D} + \frac{1}{2d_A} - \frac{1}{r} \right) \left(\frac{1}{\epsilon_\infty} - \frac{1}{\epsilon} \right) \quad (1)$$

where the donor D and the acceptor A molecules are considered as point charges at the center of spheres of radius d_D and d_A , respectively, within a continuum dielectric. The distance r corresponds to the separation between the centers of the spheres.

The definition of λ_s given by Marcus has been employed and modified during the past years by using different solvation models. Still maintaining a continuum description of the solvent, generalizations of the Marcus formula have been proposed. Most

of them are based on the concept of equilibrium and nonequilibrium solvation free energies.^{2–7} By using such quantities, the solvent reorganization energy for a given ET reaction taking place in an environment described as a dielectric continuum and leading from the reactants R to the products P, can be defined in a general way as

$$\lambda_s^P = G_{P(R)}^{\text{neq}} - G_P^{\text{eq}} \quad (2)$$

where both nonequilibrium and equilibrium free energies refer to the final P state but they differ in the polarization due to the environment. In particular, for the nonequilibrium description, the portion that is related to the slow degrees of freedom of the solvent is kept fixed to that induced by the previous R state, while the portion related to the fast degrees of freedom is equilibrated the final P state. We note that a parallel expression of λ_s can be given in terms of $G_{R(P)}^{\text{neq}}$ and G_R^{eq} , which are the terms analogous to $G_{P(R)}^{\text{neq}}$ and G_R^{eq} , with the roles of R and P exchanged: This parallel expression is related, in the Marcus picture of the ET, to the curvature of the parabola of the reactant state instead of to that of the product state.

The definition of the equilibrium and nonequilibrium solvation free energies entering in eq 2 is based on the specific solvation model used (see ref 8 for a recent review). In the present work, the definition used is based on the integral equation formalism (IEF)⁹ version of the polarizable continuum model.^{8,10} In this approach, the solute is represented as a quantum mechanical charge distribution inside a cavity of molecular shape immersed in a macroscopic dielectric continuum with known permittivity. The electrostatic interactions between solute and solvent can then be represented in terms of an apparent surface charge on the cavity, which produces a perturbation to the solute wave function, translated as an operator

^{*} To whom correspondence should be addressed. (M.C.) Present address: Department of Chemistry, Yale University, 225 Prospect St., New Haven, CT 06520-8107. E-mail: marco.caricato@yale.edu. (F.I.) E-mail: fingrosso@gmail.com.

[†] Università di Pisa.

[‡] École Normale Supérieure.

[§] Kyoto University.

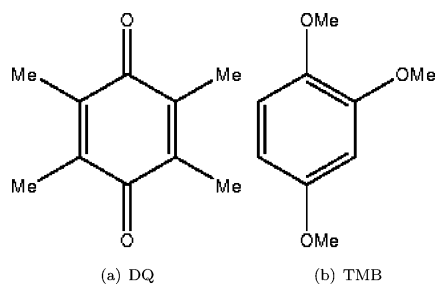


Figure 1. Structures of DQ and TMB.

to be added to the solute Hamiltonian. The solution of the resulting quantum mechanical problem gives the solute wave function modified by the solvent in a mutually polarized way and the corresponding equilibrium (or alternatively nonequilibrium) free energies determining λ_s through eq 2.

As far as experiments are concerned, a novel method to investigate the λ_s for photoinduced ET systems using time-resolved electron paramagnetic resonance (TREPR) spectroscopy was developed^{11–14} and applied to study ET reactions in polar solvents. In particular, in ref 14, the role of the solvent in ET between solvated species was investigated with attention to solvents that can give intermolecular hydrogen bonds with one of the solutes. The system considered was a solvent-separated radical ion pair (RIP), in which the charge separation was the result of a photoinduced intermolecular process. The solvent-separated ion pair was composed by duroquinone (DQ) and 1,2,4-trimethoxybenzene (TMB) (see Figure 1) and the ET reaction involved an electron passing from the donor (TMB) to the acceptor (DQ): $\text{DQ} + \text{TMB} \rightarrow \text{DQ}^- + \text{TMB}^+$.

The conclusion of that work was that, when compared to experimental results, the theoretical predictions from Marcus's theory cannot correctly reproduce the solvent reorganization energy in the presence of the solute–solvent hydrogen bond.

In the present study, this experimental evidence is analyzed by using the IEFPCM approach coupled to density functional theory (DFT) and complete active space self-consistent field (CASSCF²²) calculations on both noninteracting and interacting DQ and TMB pairs in different solvents. In the first part of the study, we evaluated the contribution to the solvent reorganization energy due to each fragment of the ET reaction: the two processes $\text{DQ} \rightarrow \text{DQ}^-$ and $\text{TMB} \rightarrow \text{TMB}^+$ are thus studied by two different series of calculations in solution. The solvents that we considered are the same as in the experimental work in ref 14, such as pure polar solvents and mixtures, which, in the continuum approach, were represented by their (static, optical) dielectric constants. In particular, calculations were performed in pure methanol (MeOH), dimethyl sulfoxide (DMSO), *N,N*-dimethylformamide (DMFA), and in mixtures of DMSO with benzonitrile (PhCN) and MeOH with PhCN. Whenever the presence of specific solute–solvent interactions could represent an important contribution to the interaction energy, we explicitly included solvent molecules in the solute cavity. In this particular case, the supermolecular calculation had the purpose of evaluating the hydrogen bond contribution to the interaction energy for charged DQ immersed in MeOH. We also confirmed the importance of the hydrogen bond between the DQ and the MeOH solvent by providing results of solute–solvent pair distribution functions obtained by means of a modified version of RISM-SCF calculations.²³

The second part of the paper is dedicated to calculations of the RIP in solution. The calculations were run at different intermolecular distances and for different conformations of the cluster. To our knowledge, this represents the first example of

TABLE 1: Static and Optical Dielectric Constants Used in the Calculations

	ϵ	ϵ_∞		ϵ	ϵ_∞
DMFA	36.71	2.039	PhCN	25.20	2.329
DMSO	46.45	2.184	DMSO/PhCN	44.32	2.199
MeOH	32.66	1.761	MeOH/PhCN	25.65	2.295

a quantum calculation on a large system in a continuum solvent for ET studies.

This paper is organized as follows. Section 2 contains the description of the methodology and of the calculations run in this work. In Section 2.2, results on the isolated fragments in solution are presented and discussed. Similarly, Section 2.3 contains the results for the ET reaction within the RIP in solution. Finally, in Section 3, we summarize the most important findings obtained through our investigation.

2. ET between RIP

2.1. Computational Details. Calculations for the single fragments have been run at the DFT level with Gaussian 03.¹⁵ The B3LYP hybrid functional by Becke, based on the exchange–correlation functional by Lee, Parr, and Yang, was employed in the calculations.¹⁶ In the case of charged species, spin-unrestricted calculations were performed. The basis set used was a 6-311++G(d,p) basis set.

For all species, geometry optimizations in solution preceded each calculation. We considered pure solvents, such as MeOH, DMFA, and DMSO, and mixtures of DMSO with PhCN (the molar fraction of DMSO was $\chi_{\text{DMSO}} = 0.9$) and of MeOH with PhCN ($\chi_{\text{MeOH}} = 0.6$), indicated as DMSO/PhCN and MeOH/PhCN, respectively. The sphere radii¹⁷ used to build the molecular cavity were equal to 1.9 Å for CH, 2.0 Å for CH_n ($n = 2, 3$), 1.7 Å for other C, 1.52 Å for O, 1.6 Å for N, and 1.2 Å for H when bonded to N, all multiplied by a cavity size factor of 1.2.

To calculate the dielectric constant of the mixtures, we assumed that it is possible to express both ϵ and ϵ_∞ of the mixture as a linear combination of the values for the pure liquids (indicated as 1 and 2):

$$\epsilon(\text{mix}) = \chi_1 \epsilon(1) + \chi_2 \epsilon(2)$$

$$\epsilon_\infty(\text{mix}) = \chi_1 \epsilon_\infty(1) + \chi_2 \epsilon_\infty(2) \quad (3)$$

where χ_i is the molar fraction of component i of the mixture. The values of the dielectric constants for liquids¹⁸ and mixtures are reported in Table 1.

For all of the solvents and the mixtures, the solvent reorganization energy was calculated as the difference of equilibrium and nonequilibrium free energies (see eq 2) where G^{eq} and G^{neq} were defined as described in ref 6.

In the case of MeOH, we investigated the effects of intermolecular hydrogen bond formation with the anionic form of DQ. In this case, one or two solvent molecules were included in the cavity and new geometry optimizations were performed. Moreover, to calculate the energetic contribution due the hydrogen bond in the DQ^- –MeOH complex, we used the definition based on a supermolecular approach.¹⁹ According to this definition, the hydrogen bond energetic contribution can be evaluated from the binding energy of the complex and the energies of the anion and of a MeOH molecule as:

$$E^{\text{HB}} = E^{\text{complex}} - [E^{\text{MeOH}} + E^{\text{DQ}^-}] \quad (4)$$

In addition, the basis set superimposition error²⁰ (BSSE) correction was included in the calculation of the binding energy by employing the counterpoise²¹ method. This error arises when dealing with finite basis sets: In the complex, the internal energy of each monomer is lowered by the use of the basis orbital of the other monomer, unless a very large basis set is used. By including the BSSE correction, the final form of eq 4 becomes

$$E^{\text{HB}} = E^{\text{complex}} + \delta E^{\text{BSSE}} - [E^{\text{MeOH}} + E^{\text{DQ}^-}] \quad (5)$$

This expression can be easily generalized for more than one solvent molecule. The calculation of the BSSE correction was performed for the systems in vacuo, and we assumed that the same correction is also valid for the solvated systems.

Calculations on the clusters were performed at the CASSCF level. The choice of this level of calculation is due to the fact that the UB3LYP functional (where U stands for “unrestricted”) failed to describe the charge separation in the whole cluster system. We used the same basis set and the same cavity parameters used for the single-fragments calculations. The complete active space holds four electrons and four orbitals (two occupied and two virtual), obtained by a preliminary calculation at Hartree–Fock level in vacuo. The choice of the orbitals in the CAS was made to ensure that the occupied ones were mainly localized on the TMB fragment, whereas the virtual ones were mainly located on the DQ fragment. The charge transfer was obtained by considering a triplet multiplicity for the overall system. By following this procedure, in all of the cases considered, the main configuration (with a weight larger than 99.99%) involved a highest occupied molecular orbital (HOMO)–lowest unoccupied molecular orbital (LUMO) excitation. In particular, the HOMO is represented by a π orbital on the TMB fragment, and the LUMO is represented by a π^* orbital on the DQ fragment. Even though the shape of these orbitals changes slightly for different calculations (in which we vary the solvents, the intermolecular distances, and the mutual orientation of the RIP), the nature of the orbitals remains the same as well as the nature of the ET process ($\pi_{\text{TMB}} \rightarrow \pi_{\text{DQ}}^*$).

The same geometries employed in the single fragments calculations were also used in the cluster. A geometry optimization for such a large system in solution at the CASSCF level and with a 6-311++G(d,p) basis set would in fact be very demanding from a computational viewpoint. However, this is not expected to be a drastic approximation, since the fragments that we studied have quite rigid structures. In addition, we recall that the orbitals involved in the ET process are mainly located on the molecular rings. Therefore, the changes in the geometries of the two molecules should not affect to a large extent the values of the solvent reorganization energy. Other geometrical parameters, such as the distance between the fragments and the relative orientation with respect to each other, are analyzed by letting these parameters vary and by subsequently performing single-point calculations, as explained below. The results obtained with this procedure are analyzed in Section 2.3.

The cluster calculations were performed at various distances (100, 50, 13, 12, 11, and 10 Å) between the centers of the benzene rings of DQ and TMB molecules. The two largest intermolecular distances allowed us to simulate the situation of two isolated fragments, whereas the others were chosen as a range centered on the value proposed in ref 14 as the distance at which the ET occurs. As no information about the relative orientation of the fragments is available, a statistical analysis should be introduced by using, for example, data extracted from molecular dynamics simulation or similar approaches generating

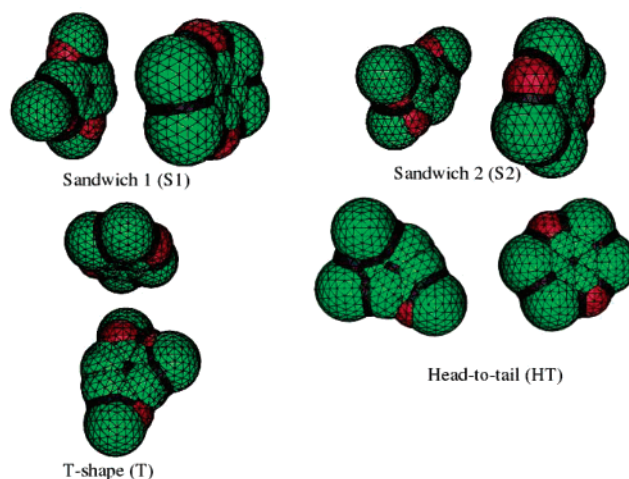


Figure 2. Four different configurations chosen for the cluster calculation in a solvent continuum. The two solutes, DQ and TMB, are shown as embedded in a representative IEFPCM cavity.

TABLE 2: Solvent Reorganization Energies (eV) in Pure Solvents and in Mixtures

	$\lambda_s^{\text{exp } a}$	$\lambda_s^{\text{M } b}$	λ_s^c	λ_s^c	$\lambda_s^{\text{tot } d}$
	DQ-TMB	DQ-TMB	DQ	TMB	DQ-TMB
DMFA	1.28 (± 0.02)	1.32	0.93	0.91	1.84
DMSO		1.24	0.88	0.85	1.73
MeOH		1.53	1.07	1.04	2.11
DMSO/PhCN	1.26 (± 0.02)	1.23	0.87	0.85	1.72
MeOH/PhCN	1.36 (± 0.02)	1.13	0.80	0.78	1.58

^a The experimental values of λ_s were taken from ref 14. ^b λ_s^{M} was obtained with the Marcus expression (eq 1) at 13 Å. ^c Values of λ_s for the fragments were obtained with IEFPCM at DFT level. ^d Values of λ_s^{tot} were obtained as the sum of the λ_s values for the fragments.

a large number of independent configurations. Here, however, we defined four configurations (two of “sandwich” type, S1 and S2, one of T-shape, T, and a “head-to-tail” one, HT), as representative of possible interactions between the two ions. These are reported in Figure 2, where they are shown as embedded in the corresponding IEFPCM cavities. The differences in the solvent reorganization energies for the various configurations at a fixed distance between the fragments will be used to analyze the relative importance of the orientation with respect to the distance between the molecules, as reported in Section 2.3.

2.2. Single Fragments. Table 2 contains the calculated solvent reorganization energies for the isolated processes on the two fragments. The results were obtained through IEFPCM calculations (in pure solvents and in mixtures); we also reported the experimental data and the λ_s^{M} values calculated with the Marcus expression (see eq 1) for a comparison. The latter were obtained by using an intermolecular distance of 13 Å, which was suggested to be the distance at which ET occurs.¹⁴ The sum of the solvent reorganization energies of the two fragments, λ_s^{tot} , calculated with IEFPCM, is also reported in the table, as it represents a first approximation of the λ_s for the whole system.

As expected, for all the solutions, the sum λ_s^{tot} overestimates the experimental value. This is due to the fact that the sum of the solvent reorganization energies for the single fragments does not include the interaction term. Adding this term would lead to a smaller value of the reorganization energy, as it can be seen by considering the Marcus definition of λ_s^{M} , since it corresponds to the term $-1/r$ (see eq 1). This problem will be addressed in the next section. Here, we shall limit the discussion to qualitatively comparing the computed trend of λ_s for the single

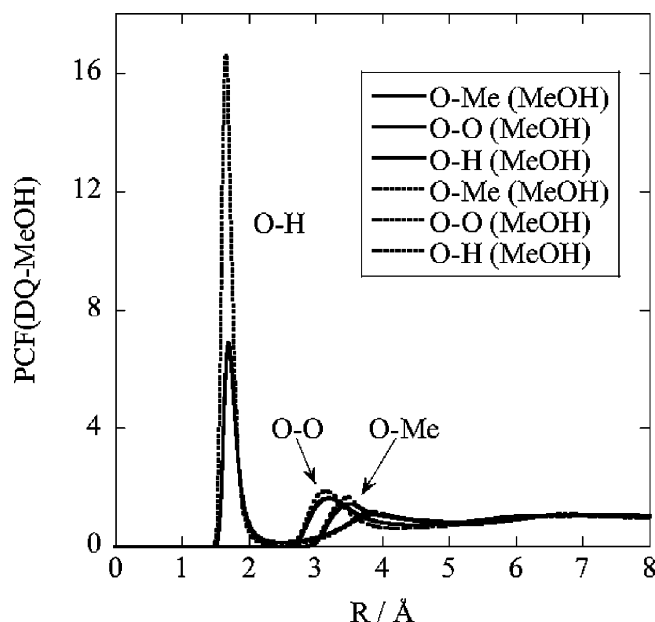


Figure 3. Solute (DQ)-Solvent pair correlation functions for the solute oxygen atoms before (full lines) and after (dashed lines) ionization.

fragments to the corresponding experimental ones as the dielectric properties of the medium change.

Passing from DMFA to DMSO, the calculated values of λ_s decrease as the experimental ones do. As for the mixture DMSO/PhCN, the situation does not change in a significative way, as the values of both ϵ and ϵ_∞ are quite similar to those of the pure solvent (the molar fraction of DMSO in this mixture is in fact close to 1, $\chi_{\text{DMSO}} = 0.9$). Thus, in pure DMSO, in DMSO/PhCN, and in DMFA, the electrostatic interaction between the solute and the solvent plays the main role.

The situation is different for MeOH and its mixture with PhCN. In fact, in these two cases, the dielectric characteristics are very different (both static and optical dielectric constants in Table 1). As shown in eq 1, λ_s is sensitive to variations of the dielectric properties, and this is confirmed by the fact that we obtained different values for λ_s^{tot} in the two cases. However, the experimental results give a larger value of λ_s in this mixture compared to DMFA and to DMSO/PhCN; we obtain the opposite trend from the calculation.

This behavior suggests that an interpretation based only on the electrostatic interaction between the solute and the solvent is not sufficient to describe the phenomenon of interest, even qualitatively. The difference between the theoretical and the experimental trend for the mixture MeOH/PhCN is in fact probably due to the formation of hydrogen bond (H bond) between the DQ^- ion and at least one MeOH molecule, as suggested in ref 14. We would like to point out that the cation species, TMB^+ , does not have sites available for hydrogen bond formation, since the positive charge is delocalized on the molecular ring. On the other hand, for the anionic species, the negative charge is mainly localized on the oxygen atoms, which represent favorable sites for formation of H bond with the MeOH solvent molecules, as confirmed by our calculations.

The formation of hydrogen bond after the ET has taken place is confirmed by studying the solvation structure of DQ by means of a modified version of RISM-SCF calculations.²³ Results are presented here for DQ immersed in MeOH. More details about the computation will be presented in ref 24. In Figure 3, we report the solute-solvent (DQ-MeOH) site-site pair correlation functions for the solute oxygen atoms.

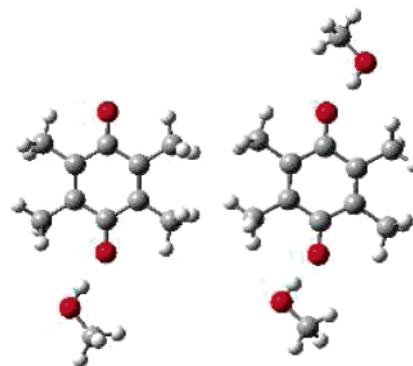


Figure 4. DQ molecule shown with one or two hydrogen-bonded molecules of MeOH.

Before ET takes place, the DQ molecule is surrounded by MeOH molecules, which give rise to the pair correlations shown in full lines. After ET, the DQ molecule is negatively charged and therefore strongly acting as hydrogen bond acceptor with respect to the MeOH molecules. At the same average O (solute)-H (solvent) distance (about 1.8 Å), the oxygen sites of the charged molecule experience a large increase of MeOH-hydrogen sites density. Such a distance is consistent with intermolecular hydrogen bond, and the fact that the position of the first peak in the (solute)-O--(solvent)-H pair distribution function stays the same before and after ionization seems to be an indication of small changes in the first solvation shell in terms of relative solute-solvent distances. The probability of hydrogen bond formation around DQ^- is therefore much higher than it is for the corresponding neutral species. Because RISM-SCF results strongly suggest the presence of intermolecular hydrogen bond and that the probability for such a bond to be present is different before and after ET, we decided to take explicitly into account hydrogen-bonded solvent molecules in our calculations.

To investigate the importance of the hydrogen bond contribution to the reorganization energy, we performed calculations on the clusters formed by one or two MeOH molecules and DQ^- , shown in Figure 4.

The values of λ_s obtained for the two clusters are different. When only one solvent molecule was considered, we obtained a value of $\lambda_s = 0.81$ eV, which is quite similar to the result reported in Table 2. This fact can be explained by considering that the solvent molecule covers only one of the negatively charged regions of the anion (i.e., those around the oxygen atoms); thus, the dielectric response on the other region is similar to the case where no explicit solvent molecules were introduced. To obtain the correct reorganization energy, this value needs to be added to the energetic contribution arising from the intermolecular H bond, according to eq 5. The result found for E^{HB} was 0.25 eV; thus, the final value of the reorganization energy associated to $\text{DQ} \rightarrow \text{DQ}^-$ in MeOH/PhCN becomes 1.06 eV, which now qualitatively follows the experimental trend.

When we included another MeOH molecule, the value of λ_s significantly changed, passing to 0.49 eV. This time, the explicit solvent molecules cover both the negatively charged regions of the solute molecule; thus, the dielectric effect becomes smaller. In this case, the H bond contribution is $E^{\text{HB}} = 0.51$ eV. Finally, the total value of $(E^{\text{HB}} + \lambda_s)$ is equal to 1.00 eV, which is almost equivalent to that obtained with a single MeOH molecule.

From this analysis, we can conclude that the contribution of the H-bond plays a central role in the definition of the solvent reorganization energy in protic polar solutions. However, by

TABLE 3: Reorganization Energies (eV) for the RIP^a in DMFA

<i>d</i> (Å)	10	11	12	13	50	100
S1	1.26	1.31	1.36	1.40	1.76	1.83
S2	1.25	1.31	1.36	1.39	1.76	1.83
T	1.22	1.28	1.33	1.38	1.76	1.83
HT	1.23	1.29	1.34	1.38	1.76	1.83

^a The experimental value is 1.28 ± 0.02 eV.¹⁴

considering only the energetic contributions, no information can be obtained about the number of solvent molecules forming hydrogen bonds with the solute molecule in its anionic form, and a further use of other techniques, such as molecular dynamics computer simulations, would be desirable.

By using calculations performed with the IEFPCM continuum model, we confirmed that the solvent plays a major role for ET in RIPs. For polar solvents, this role can be described in terms of electrostatic interactions. We also showed that these are not always sufficient when specific solute–solvent interactions give rise to additional contributions to the solvation energy and consequently to the reorganization energy. In these cases, refinements in the model are necessary, as described in the second part of this paper, in which we shall discuss results obtained for ET in the ionic-pair cluster in solution, and more quantitative analysis will be presented for the comparison between our results and experimental measurements of the solvent reorganization energy.

2.3. Ionic-Pair Clusters. In this section, we discuss the results obtained for the clusters constituted by the RIP at different distances and four configurations (see Figure 2). These calculations represent a first attempt to recover the contribution to λ_s , which has not been considered to compute the results reported in the previous section. We recall that such a contribution corresponds to the $1/r$ term in Marcus's eq 1. This term accounts for the interaction between the two molecules exchanging one electron in the ET reaction.

We shall use results in DMFA to illustrate the discussion; thus, more details will be presented in this case. Results in other solvents will also be provided and compared to experiments.

Table 3 summarizes the DMFA results at different intermolecular distance d . We recall that calculations were performed at the CASSCF level with a 6-311++g(d,p) basis set and with an active space holding four electrons in four orbitals.

We start the analysis of the results from the value computed for an intermolecular distance corresponding to 100 Å. As shown in Table 3, at this large distance, we obtain the same value of λ_s for all of the configurations. This is not unexpected if we consider that no interactions occur in the pair separated by such a large intermolecular distance; thus, no differences should be found for different orientations. We also note that the value of 1.83 eV is almost the same value that was obtained by adding the values of the two isolated fragments calculated at DFT level (see Table 2). This confirms that λ_s is a solvent-dependent property, just slightly influenced by the level of the QM calculation used for the solute when the same basis set is used. The situation slightly changes at 50 Å; in fact, at this distance, an interaction between the RIP starts to be present, even though the different orientation between the two molecules does not significantly influence the value of λ_s .

The interaction between the fragments becomes relevant at smaller distances (10–13 Å). First, we note that the values of the reorganization energy for all configurations are much closer to the experimental one (1.28 ± 0.02 eV)¹⁴ than are the results shown in Table 2, corresponding to the sum of the values

obtained for the two fragments. The cluster approach therefore succeeded in representing the effect of the interaction between the anion and the cation on the solvent reorganization process caused by ET in the pair.

Second, we observed that the values of λ_s for the four clusters are different. The relative orientation of the two molecules affects the value of the solvent reorganization energy, even though this variable does not affect the value of λ_s as much as the distance between the fragments. This behavior suggests that, even though a molecular dynamics study of the relative orientation between the two molecules would be desirable, it is not strictly necessary for an evaluation of the distance at which the ET process occurs.

By analyzing the results in Table 3, we observe that at each distance (except for 100 and 50 Å, for the reasons that we mentioned above), the configurations S1 and S2 present values of λ_s that are closer to each other than to the ones corresponding to configurations T and HT. This is due to the similarity between the S1 and S2 configurations. Furthermore, configurations T and HT show smaller λ_s values as compared to the other two configurations, even though the π electron densities in S1 and S2 are in a more favorable orientation for the interaction. The explanation for this behavior is that the distance between the fragments is defined with respect to the centers of the benzene rings, as explained in Section 2.1, and therefore, the ring substituents in configurations T and HT are closer than in configurations S1 and S2 (see Figure 2), leading to a stronger interaction between the RIP. From the comparison between configurations T and HT, we also observe that the interaction between the fragments is stronger in configuration T than in HT, possibly because in the latter the π electron densities on the benzene rings are in a less favorable orientation for the interaction.

However, we note that even the smallest distance (10 Å) is still possibly large enough for the two molecules to move relatively freely with respect to each other (the differences in the equilibrium free energy values of the different fragments are negligible, of the order of 10^{-2} kcal/mol).

The analysis of calculations run for different cluster configurations can be summarized by saying that the distance between the fragments is the parameter that mostly influences the value of the reorganization energies. Differences between different configurations become more evident as the distance between the fragments decreases. However, these differences, which are due to different interactions between the π electron densities on the molecular rings, are still small enough to require the evaluation of λ_s as an average over all of the possible configurations, at a given distance.

Finally, we analyze the distance that better agrees with the experimental results. In ref 14, a distance of 13 Å was proposed as the one at which ET occurs, based on Marcus' formula, eq 1. In our case, such a distance seems to be too large. In fact, if we compare the results obtained at different distances with the experimental result, better agreement is found in a range between 10 and 11 Å. This confirms that, even though Marcus' formula provides a very simplified description of the phenomenon, it is able to provide results close to those obtained with a more accurate QM model, if nonspecific solute–solvent interactions occur. We would like to remark that the distances that we obtained, for all of the solvents considered, should not be taken as a quantitative determination of the distance at which the ET occurs. To achieve quantitative conclusions on such a distance, other effects should be taken into account, i.e., the geometry relaxation of the fragments or the dynamical behavior of the

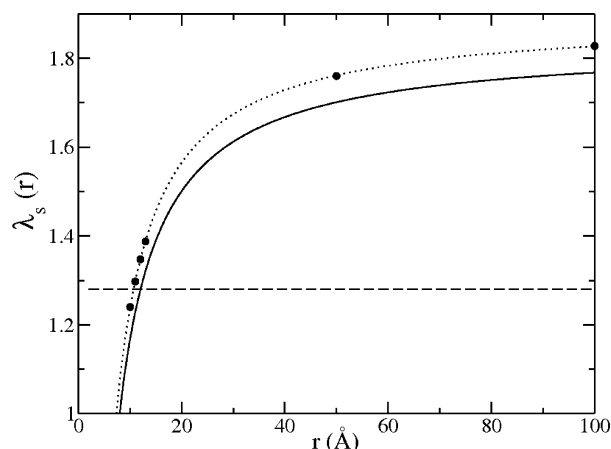


Figure 5. Fit of an average of the calculated solvent reorganization energies (full circles) with an equation of the form $f(r) = a/r + b$ (dotted line). The full line refers to the result obtained by using Marcus' equation (eq 1). The experimental result¹⁴ is shown as a reference as a dashed line.

TABLE 4: As in Table 2, Reorganization Energies (eV) for the RIP in DMSO/PhCN^a

d (Å)	11	12	13	100
S1	1.24	1.28	1.31	1.72
S2	1.24	1.28	1.29	1.72
T	1.21	1.26	1.30	1.72
HT	1.23	1.28	1.31	1.72

^a The experimental value is 1.26 ± 0.02 eV.¹⁴

molecules in solution. These effects will be considered in future extensions of this work.

In Figure 5, we report the result obtained by fitting cluster λ_s values (averaged over the different configurations) with a function, which reproduces the r dependence of the Marcus' definition (being r the distance between the donor and the acceptor): $f(r) = a/r + b$. We obtained the following values for the fitting parameters: $a = (-6.54 \pm 0.05)$ eV Å, and $b = (1.89 \pm 0.01)$ eV. The fitting curve is compared to the curve obtained by applying the definition in eq 1 and the values in Table 1.

This figure shows the effectiveness of the simple Marcus' formula in the calculation of the solvent reorganization energy when the electrostatic interaction is the main solute–solvent interaction term. From another point of view, this figure shows the capability of IEFPCM to reproduce the correct behavior of λ_s as a function of the distance between the reactants. Our curve, obtained only by computing energy differences (see eq 2), has the same shape of the curve obtained by Marcus' formula in eq 1.

Passing now to the DMSO/PhCN mixture, we observe a better agreement with experimental results at distances slightly larger than in DMFA solution, namely, between 11 and 12 Å. Results are reported in Table 4.

Similar considerations to the DMFA case can be done for this mixture. In fact, also for this solution, λ_s is less sensitive to differences between configurations than to the intermolecular distance. At 100 Å, we obtained the same results for all of the configurations, with a value that is in agreement with the λ_s^{tot} for this solution, reported in Table 2. The same analysis for the relative differences between the various configurations done for the DMFA solution could be repeated in this case.

We also qualitatively discuss the results obtained for the cluster immersed in MeOH/PhCN. Because we did not explicitly include solvent molecules in the calculations, the results

obtained in this mixture are less accurate than the results obtained in DMFA and in DMSO/PhCN. However, some information can still be obtained.

If we only include the two RIP molecules in the solute cavity, the values of λ_s vary from an average of 1.13 eV at 11 Å to an average of 1.20 eV at 13 Å (the average is calculated over the different configurations). The long-distance value (1.58 eV) is in agreement with λ_s^{tot} reported in Table 2 for this solution. As shown before, to make the comparison with experiment more quantitative, one would need to evaluate the H-bond interaction with one (and two) explicit solvent molecule(s) in the cluster by repeating the same procedure used on the DQ fragment and apply it to the extended cluster in different mutual configurations of the two interacting molecules. This is a very extensive computational study whose realization would go beyond the scope of the present study. Here, we obtained a qualitative estimate of these effects by adding the explicit H-bond contribution as evaluated in Section 2.2 for the DQ fragment and one MeOH molecule (0.25 eV). This procedure can in fact be justified by considering that, as shown in the Single Fragments section, the polarization effect due to a single explicit solvent molecule should not affect λ_s ; thus, we can still use the average value of 1.13 eV as a valid value also for the H-bonded cluster. By adding it to 0.25 eV, which is the value of E^{HB} calculated in the previous section, we obtained an averaged result of 1.38 eV, which is in good agreement with the experimental value of 1.36 eV.

3. Concluding Remarks

We presented a work based on quantum calculations on a radical-ion pair in continuum solvents and mixtures. The method that we used is based on the application of the nonequilibrium formulation of the IEFPCM, to evaluate the solvent reorganization energy arising from ET in the RIP.

Results were provided for the solvent reorganization energy associated with changes in each of the fragments. In addition, the ET process was modeled by means of nonequilibrium quantum calculations on the cluster formed by the ionic pair.

Our investigation showed that, by means of IEFPCM calculations, the solvent effect on ET reactions can be reasonably described. This is confirmed by comparing our results with experimental data.¹⁴

We showed that it is possible to obtain agreement with experiment also in those cases in which specific effects affect the value of the solvent reorganization energy. In our model, this was accomplished by explicitly including MeOH molecule hydrogen bonded to one of the solutes in the cavity utilized for the quantum calculation.

The use of IEFPCM in the evaluation of the solvent reorganization energy allows us to obtain a more detailed description of the electron/charge transfer between two molecules (or between two parts of the same molecule) with respect to previous approaches. Specific solute–solvent interactions can not only be studied, but also, the role of relative orientations between donor and acceptor, the effect of specific chemical groups in the solutes, or that of the solutes orbitals involved in the charge transfer. This information is lost in simplified models.

Acknowledgment. Financial support by Gaussian Inc. and by the Max Born Institut für Nichtlineare Optik und Kurzzeitspektroskopie for a fellowship to F.I. is acknowledged. H.S. acknowledges financial support by the Grant-in-Aid for Encouragement of Young Scientists (17750012) from the Ministry of Education, Culture, Sports, Science and Technology (MEXT) Japan.

References and Notes

- (1) Marcus, R. A. *J. Chem. Phys.* **1956**, *24*, 966.
- (2) (a) Kim, H. J.; Hynes, J. T. *J. Chem. Phys.* **1990**, *93*, 5194. (b) Kim, H. J.; Hynes, J. T. *J. Chem. Phys.* **1990**, *93*, 5211. (c) Kim, H. J.; Hynes, J. T. *J. Chem. Phys.* **1992**, *96*, 5088. (d) Gelhen, J.; Chandler, D.; Kim, H. J.; Hynes, J. T. *J. Phys. Chem.* **1992**, *96*, 1748.
- (3) Newton, M. D.; Friedman, H. L. *J. Chem. Phys.* **1988**, *88*, 4460.
- (4) (a) Basilevsky, M. V.; Chudinov, G. E.; Newton, M. D. *Chem. Phys.* **1994**, *179*, 263. (b) Basilevsky, M. V.; Chudinov, G. E.; Rostov, I. V.; Liu, Y. P.; Newton, M. D. *J. Mol. Struct. (THEOCHEM)* **1996**, *371*, 191. (c) Basilevsky, M. V.; Parsons, D. F.; Vener, M. V. *J. Chem. Phys.* **1998**, *108*, 1103.
- (5) Aguilar, M.; Olivares del Valle, F. J.; Tomasi, J. *J. Chem. Phys.* **1993**, *98*, 7375.
- (6) (a) Mennucci, B.; Cammi, R.; Tomasi, J. *J. Chem. Phys.* **1998**, *109*, 2798. (b) Cammi, R.; Mennucci, B. *J. Chem. Phys.* **1999**, *110*, 9877. (c) Cammi, R.; Mennucci, B.; Tomasi, J. *J. Phys. Chem. A* **2000**, *104*, 5631.
- (7) (a) Li, X.-Y.; Fu, K.-X.; Zhu, Q.; Shan, M.-H. *J. Comput. Chem.* **2004**, *25*, 835. (b) Fu, K.-X.; Li, X.-Y.; Zhu, Q.; Gong, Z.; Lu, S.-Z.; Bao, Z. M. *J. Mol. Struct. THEOCHEM* **2005**, *715*, 157. (c) Li, X.-Y.; Fu, K.-X. *J. Theor. Comput. Chem.* **2005**, *4*, 907.
- (8) Tomasi, J.; Mennucci, B.; Cammi, R. *Chem. Rev.* **2005**, *105*, 2999.
- (9) (a) Cancès, E.; Mennucci, B.; Tomasi, J. *J. Chem. Phys.* **1997**, *107*, 3032. (b) Mennucci, B.; Cancès, E.; Tomasi, J. *J. Phys. Chem. B* **1997**, *101*, 10506.
- (10) (a) Miertus, S.; Scrocco, E.; Tomasi, J. *J. Chem. Phys.* **1981**, *55*, 117. (b) Cammi, R.; Tomasi, J. *J. Comput. Chem.* **1995**, *16*, 1449.
- (11) Kobori, Y.; Akiyama, K.; Tero-Kubota, S. *J. Chem. Phys.* **2000**, *113*, 465.
- (12) Kobori, Y.; Yago, T.; Akiyama, K.; Tero-Kubota, S. *J. Am. Chem. Soc.* **2001**, *123*, 9722.
- (13) Yago, T.; Kobori, Y.; Akiyama, K.; Tero-Kubota, S. *J. Phys. Chem. B* **2002**, *106*, 10074.
- (14) Yago, T.; Kobori, Y.; Akiyama, K.; Tero-Kubota, S. *Chem. Phys. Lett.* **2003**, *369*, 49.
- (15) Frisch, M. J.; Trucks, G. W.; Schlegel, H. B.; Scuseria, G. E.; Robb, M. A.; Cheeseman, J. R.; Montgomery, J. A., Jr.; Vreven, T.; Kudin, K. N.; Burant, J. C.; Millam, J. M.; Iyengar, S. S.; Tomasi, J.; Barone, V.; Mennucci, B.; Cossi, M.; Scalmani, G.; Rega, N.; Petersson, G. A.; Nakatsuji, H.; Hada, M.; Ehara, M.; Toyota, K.; Fukuda, R.; Hasegawa, J.; Ishida, M.; Nakajima, T.; Honda, Y.; Kitao, O.; Nakai, H.; Klene, M.; Li, X.; Knox, J. E.; Hratchian, H. P.; Cross, J. B.; Bakken, V.; Adamo, C.; Jaramillo, J.; Gomperts, R.; Stratmann, R. E.; Yazyev, O.; Austin, A. J.; Clifford, S.; Cioslowski, J.; Ochterski, J. W.; Ayala, P. Y.; Morokuma, K.; Voth, G. A.; Salvador, P.; Dannenberg, J. J.; Zakrzewski, V. G.; Dapprich, S.; Daniels, A. D.; Strain, M. C.; Farkas, O.; Malick, D. K.; Rabuck, A. D.; Raghavachari, K.; Foresman, J. B.; Ortiz, J. V.; Cui, Q.; Baboul, A. G.; Clifford, S.; Cioslowski, J.; Stefanov, B. B.; Liu, G.; Liashenko, A.; Piskorz, P.; Komaromi, I.; Martin, R. L.; Fox, D. J.; Keith, T.; Al-Laham, M. A.; Peng, C. Y.; Nanayakkara, A.; Challacombe, M.; Gill, P. M. W.; Johnson, B.; Chen, W.; Wong, M. W.; Gonzalez, C.; Pople, J. A. *Gaussian 03*, Revision C.02; Gaussian, Inc.: Wallingford CT, 2004.
- (16) (a) Becke, A. D. *J. Chem. Phys.* **1993**, *98*, 1372. (b) Becke, A. D. *J. Chem. Phys.* **1993**, *98*, 5648.
- (17) Bondi, A. *J. Phys. Chem.* **1964**, *68*, 441.
- (18) Horng, M. L.; Gardecki, J. A.; Papazyan, A.; Maroncelli, M. *J. Phys. Chem.* **1995**, *99*, 17311.
- (19) van Lenthe, J. H.; van Duijneveldt-van de Rijdt, J. G. C. M.; van Duijneveldt, F. B. *Adv. Chem. Phys.* **1987**, *69*, 521.
- (20) Jansen, H. B.; Ros, P. *Chem. Phys. Lett.* **1969**, *3*, 140.
- (21) Simon, S.; Duran, M.; Dannenberg, J. J. *J. Chem. Phys.* **1988**, *105*, 11024.
- (22) (a) Amovilli, C.; Mennucci, B.; Floris, F. M. *J. Phys. Chem. B* **1998**, *102*, 3023. (b) Cossi, M.; Barone, V.; Robb, M. A. *J. Chem. Phys.* **1999**, *111*, 5295.
- (23) (a) Sato, H.; Kobori, Y.; Tero-Kubota, S.; Hirata, F. *J. Chem. Phys.* **2003**, *119*, 2753. (b) Sato, H.; Kobori, Y.; Tero-Kubota, S.; Hirata, F. *J. Phys. Chem. B* **108**, 11709.
- (24) Sato, H.; Yokogawa, D.; Sakaki, S.; Mennucci, B. Manuscript in preparation.